

RESEARCH ARTICLE

OPEN ACCESS 

Sodium houthuyfonate inhibits the cariogenic virulence of *Streptococcus mutans* through the downregulation of VicRK two components pathway

Yaqi Chi^{a,b}, Ye Wang^{a,b}, Di Fu^{a,b}, Lin Yao^{a,b}, Mingying Wei^{a,b}, Ge Zhou^{a,b}, Guang Yang^c, Ling Zou^{a,b} and Biao Ren^a

^aState Key Laboratory of Oral Diseases, National Clinical Research Center for Oral Diseases, West China Hospital of Stomatology, Sichuan University, Chengdu, China; ^bState Key Laboratory of Oral Diseases, National Clinical Research Center for Oral Diseases, Department of Endodontics, West China Hospital of Stomatology, Sichuan University, Chengdu, China; ^cInstitute of Biomedical Engineering, College of Medicine, Southwest Jiaotong University, Chengdu, China

ABSTRACT

Background: Caries is one of the most common diseases worldwide, and *Streptococcus mutans* is considered to be the primary cariogenic pathogen of dental caries. Sodium houthuyfonate (SH) has showed potential antibacterial effects, however, its actions and mechanisms on *S. mutans* and cariogenicity remain unclear and need further study.

Materials and Methods: we investigated the effects of SH on the cariogenic ability of *S. mutans*, including growth, biofilm formation, exopolysaccharides (EPS) and acid productions. RNA-Seq and mutants' validation were also performed to explore the mechanisms of SH on *S. mutans*. The dental caries rat model was finally employed to evaluate the anti-caries capabilities of SH.

Results: The MIC of SH against *S. mutans* was 64 µg/mL. SH inhibited biofilm formation and cariogenic virulence of *S. mutans*, including EPS and acid productions, in a dose-dependent manner. RNA-seq analysis indicated that SH significantly downregulated the VicRK pathway, a key pathway regulating biofilm formation and EPS generation. The $\Delta vicK$, $\Delta vicR$, $\Delta gtfB$ and $\Delta gtfC$ mutants were more sensitive to SH, while *VicK* and *VicR* overexpression strains *OEvicK* and *OEvicR* were more resistant to SH than WT strains, indicating that SH downregulated the VicRK pathway to inhibit the cariogenicity of *S. mutans*. SH also significantly inhibited the development of dental caries in rats without systematic toxicities. The expressions of *S. mutans VicK*, *VicR*, *GtfC* and *GtfD* genes from rat plaques were downregulated by SH.

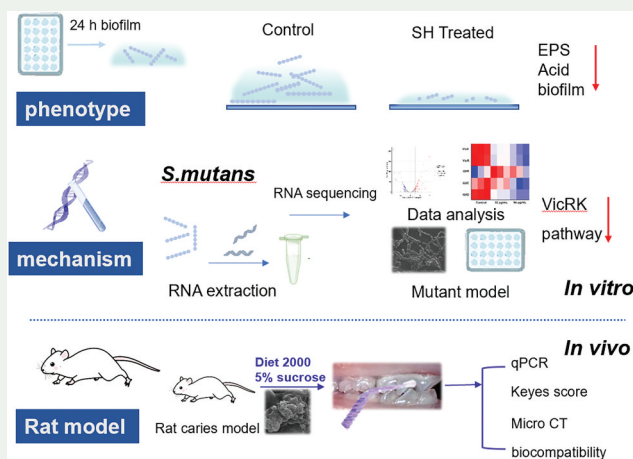
Conclusion: This study suggested SH inhibited the cariogenic virulence of *S. mutans* through the downregulation of VicRK two components pathway, thereby offering novel insights for clinical caries prevention.

ARTICLE HISTORY

Received 12 October 2024
Revised 18 January 2025
Accepted 6 February 2025

KEYWORDS

Sodium houthuyfonate;
Streptococcus mutans; caries;
virulence; RNA-seq; two
component system (VicRK)



Introduction

Caries is a hard tissue demineralization disease caused by the disorder of oral microecology [1]. According to the incomplete estimates, nearly

2.3 billion people have untreated dental caries in their mouths. The current dental caries situation, characterized by the high incidence rate and low

CONTACT Ling Zou  zouling@scu.edu.cn; Biao Ren  renbiao@scu.edu.cn  State Key Laboratory of Oral Diseases, National Clinical Research Center for Oral Diseases, West China Hospital of Stomatology, Sichuan University, No. 14 Renmin South Road, Chengdu 610041, China

 Supplemental data for this article can be accessed online at <https://doi.org/10.1080/20002297.2025.2465345>

© 2025 The Author(s). Published by Informa UK Limited, trading as Taylor & Francis Group.

This is an Open Access article distributed under the terms of the Creative Commons Attribution-NonCommercial License (<http://creativecommons.org/licenses/by-nc/4.0/>), which permits unrestricted non-commercial use, distribution, and reproduction in any medium, provided the original work is properly cited. The terms on which this article has been published allow the posting of the Accepted Manuscript in a repository by the author(s) or with their consent.

treatment rate, poses a significant challenge to public health and exacerbates the socio-economic burden [2,3]. Therefore, the prevention and treatment of dental caries is an urgent issue to be solved.

Streptococcus mutans (*S. mutans*) is considered to be the primary cariogenic pathogen of dental caries. *S. mutans* metabolizes sucrose into glucans through glucosyltransferase, while the by-product of sucrose metabolism, lactic acid, can lead to a decrease of local pH, ultimately resulting in demineralization of enamel and caries development [4]. The production of exopolysaccharides (EPS) is an essential factor contributing to the virulence of *S. mutans* [5]. It plays a key role in the biofilm formation of *S. mutans* and increase of adhesion between bacteria and teeth. EPS also promote the interactions between different bacterial species and protect the bacterial cells within oral biofilms against antibiotics and environmental pressures [6]. Hence, inhibiting the EPS production is a practical strategy for the prevention and treatment dental caries.

The effective removal of dental plaque is a critical way to reduce the development of dental caries. Except for mechanical methods, fluoride is widely used in caries control [7]. Fluoride is successful in decreasing the demineralization of tooth enamel at acidic environment [8,9], and it also showed some inhibitory activities on biofilm formation [10,11]. However, high-dose fluoride treatments are insufficient to prevent caries in individuals with high risk or those with reduced saliva flow/buffering capacity [7,12]. Fluoride has also been challenged due to its side effects, such as fluorosis of bone and induction of fluoride resistance in oral bacteria. Other methods, such as antimicrobial peptides (AMPs) and phages, have also been developed for the treatment of dental caries [13]. Natural products are potent resources for the development of bioactive agents against different diseases [14], due to their natural structures, diverse functionalities, cost-effectiveness and so on [15].

Houttuynin [$\text{CH}_3(\text{CH}_2)_8\text{COCH}_2\text{CHO}$], a primary and potent phytoanticipin obtained from the plant *Houttuynia cordata* Thunb, belongs to the Saururaceae family. Sodium houttuuyfonate (SH, $\text{CH}_3(\text{CH}_2)_8\text{COCH}_2\text{CHOHSO}_3\text{Na}$, Figure 1a) is a derivative synthesized from houttuynin and sodium bisulfite [16,17]. SH showed multiple activities

against pneumonia [18], bronchitis [19], and urinary tract infections [20], and SH also proved its antimicrobial activities on different species. Ye et al. reported that the SH could inhibit *Bacillus subtilis* through the hydrophobic interactions between SH and membrane proteins [21]. Shao et al. reported that SH inhibited the quorum sensing system, flagella and pili formation and dispersion of *Pseudomonas aeruginosa* [22]. Wang et al. reported that SH regulated the nucleic acid metabolism of *Candida albicans* and synergized with other antifungals against fungal growth [23]. Currently, the actions and mechanisms of SH on *S. mutans* and its cariogenicity remain unclear. Therefore, the anti-*S. mutans* and its cariogenicity of SH were evaluated through growth, biofilm formation, EPS and acid productions and dental caries rat model in this study. RNA-Seq analysis and the key gene mutants were also employed to investigate the mechanisms of SH on *S. mutans*.

Materials and methods

Stains, growth condition and compounds

S. mutans UA159 was obtained from the American Type Culture Collection (ATCC, USA). The *VicK*, *GtfB* and *GtfBC* null mutant ($\Delta vicK$ [24,25], $\Delta gtfB$ [26] and $\Delta gtfBC$ [26]), Anti-sense *VicR* strain (*ASvicR*) [25,27], and over-expression (*OE vicK*) [24], *OEvicR* strains [28] were also employed to confirm the drug effects on *VicRK* pathway. *ΔvicK*, *ASvicR* and *OEvicK* were kindly provided by professor Lei Lei, and *OEvicR*, *ΔgtfB* and *ΔgtfBC* were kindly provided by professor Li Yuqing (State Key Laboratory of Oral Diseases, Sichuan University, Chengdu, China). The strains maintained at 50% glycerol stocks ($-80\text{ }^\circ\text{C}$) were plated on brain heart infusion (BHI) agar plate and cultured under anaerobic conditions (10% CO_2 , 10% H_2 , and 80% N_2) at 37°C for 24 h. Single colony was selected to incubate in BHI liquid medium for overnight cultivation. The culture was diluted 20 times and grew in fresh BHI until optical density ($\text{OD}_{600\text{nm}} = 0.5$ (logarithmic growth phase). Diluted 100 times with BHI medium (if biofilm culture, use BHIS (BHI with 1% (*w/v*) sucrose added) for subsequent experiments. SH was purchased from Xi'an Kai

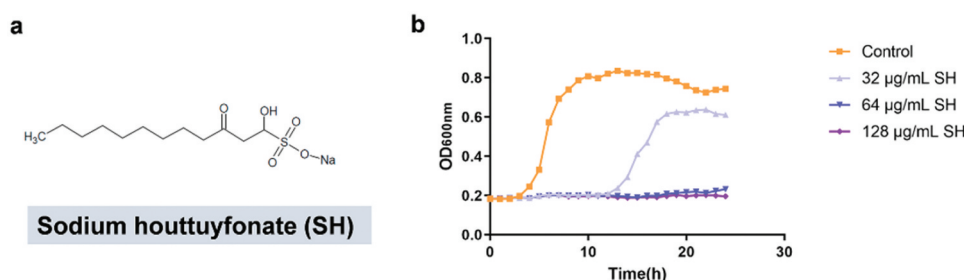


Figure 1. (a) The molecule structure of SH. (b) Growth curves of *S. mutans* under SH treatments.

Lai Biological Engineering Co., Ltd (Xi'an, China), with the purity $\geq 98\%$.

Determination of minimum inhibitory concentration (MIC)

Conventional broth microdilution method was used to measure MIC. SH was dissolved by BHI under heating and diluted through twice echelon dilution method. Bacterial suspension ($100\ \mu\text{L}$, $\text{OD}_{600\ \text{nm}} = 0.5$ diluted 50 times) and the diluted SH $100\ \mu\text{L}$ were added to each well of the 96-well microplate. The results were observed after 24 h anaerobic incubation, and the MIC was defined as the lowest concentration that the well looked clear and transparent. After 24 h incubation, the medium in 96-well microplate was sub-cultured to the BHI plate. The MBC was considered to be the lowest concentration of the SH in which microbial growth was not observed.

The follow-up phenotypic assays were divided into four groups: the final SH concentrations of 1/2 MIC, MIC, 2MIC and negative control (BHI). Each phenotypic assays comprised of three parallel groups, and each was replicated three times.

Growth curve assay

The bacterial suspension ($100\ \mu\text{L}$, $\text{OD}_{600\ \text{nm}} = 0.5$ diluted 50 times) was mixed with BHI medium containing gradient concentration drugs, resulting in a final drug concentration of 0, 1/2MIC, MIC, 2MIC. Then, the 96-well plate was incubated anaerobically at 37°C for 24 h, and measured the $\text{OD}_{600\ \text{nm}}$ of bacterial solution every 1 h by the microplate reader (Thermo Fisher, Waltham, MA, USA).

Biofilm formation assay

The bacterial suspension ($500\ \mu\text{L}$, $\text{OD}_{600\ \text{nm}} = 0.5$ diluted 50 times) was mixed with BHIS medium containing gradient concentration drugs, resulting in a final drug concentration of 0, 1/2MIC, MIC, 2MIC. Then, the 24-well plate was incubated anaerobically at 37°C for 24 h.

Crystal violet (CV) staining assay

CV assay was used to measure the biofilm biomass. The overnight biofilm was softly washed by phosphate-buffered saline (PBS, pH 7.2–7.4, Solarbio Biotech, China). Next, fixed the biofilms with 2.5% glutaraldehyde for 15 min. Then, the biofilm was stained with 0.1% crystal violet for 10 min and washed by PBS. Acetic acid (33%) was used to resolubilize the dyed biofilm for 30 min. The eluent was added to a new 96-well plate and the absorbance was detected at $\text{OD}_{600\ \text{nm}}$ by the microplate reader [29].

Colony-forming units (CFU) assay

Biofilm was washed by PBS softly to remove the planktonic cells. The biofilm was then scraped off from the plate using the pipette tip. The cultures were resuspended in sterile PBS. The samples were vortexed and ultrasonicated at a power setting of 9 W, three times, 10 s each time according to our previous publication [29]. Then, the suspension underwent a series of dilutions (1:10) and was subsequently plated onto BHI agar plates. Plates were cultured anaerobically at 37°C for 24 h, after which the colony-forming units/mL was counted [29].

Scanning electron microscopy (SEM)

The biofilm was inoculated onto the glass slides in a 24-well microplate. Each specimen was softly washed with PBS. Subsequently, the specimens were subjected to overnight fixation at 4°C using 2.5% glutaraldehyde and dehydrated with ethanol solutions (30%, 50%, 70%, 80%, 90%) for 15 min at each stage. Then, the samples were immersed in 100% ethanol for 1 h, followed by desiccation and a gold-palladium sputter coating. The specimens were observed by SEM [29] (FEI, Hillsboro, USA) at magnifications of $1000\times$ and $20,000\times$.

Confocal laser scanning microscopy (CLSM)

The biofilm was inoculated onto the glass slides in a 24-well microplate. The samples were washed by PBS and stained by LIVE/DEAD1 BacLight™ Bacterial Viability Test Kit (L-7012, Molecular Probes™, Invitrogen, Carlsbad, CA, USA). The CLSM (Nikon AIR MP+, Japan) equipped with a $60\times$ oil immersion objective lens. Live cells were stained with SYTO 9 (excitation, 488 nm), while dead cells were stained with propidium iodide (excitation, 543 nm). Each sample was scanned for three randomly selected locations, the thickness of biofilm was analyzed by the software NIS elements viewer 4.20.

Virulence factor assays

The bacterial suspension ($500\ \mu\text{L}$, $\text{OD}_{600\ \text{nm}} = 0.5$ diluted 50 times) was mixed with BHIS medium containing gradient concentration drugs, resulting in a final drug concentration of 0, 1/2MIC, MIC, 2MIC (initial adherence assay without 2MIC).

Initial adherence assay

At the 1st, 2nd, 4th h, the biofilm was washed by PBS and then scraped and resuspended in PBS. The absorbance was detected at $\text{OD}_{600\ \text{nm}}$ by the microplate reader. The initial adherence rates were identified following the formula: Anti-adherence percentage = $(\text{OD}_{600\ \text{nm}}$ of control group – $\text{OD}_{600\ \text{nm}}$ of SH treated group) / $\text{OD}_{600\ \text{nm}}$ of control group $\times 100\%$.

Anthrone assay

The 24-well plate was incubated anaerobically at 37°C for 24 h. The biofilm was washed by PBS. Then, added 1 mL 0.4 mol/L NaOH to each well, and oscillated samples at 37°C for 2 h. Biofilm was scraped from the well and centrifuged (4,000 rpm, 10 min, 4 °C). The supernatant (0.3 mL) was combined with 0.2% anthrone-sulfuric acid reagent (0.9 mL). After water bathing (96 °C, 6 min) and cooling down to room temperature, OD_{625 nm} of each sample was measured [30].

Acid production measurement

The initial pH of the culture medium was adjusted to 7.2. Then, the pH of the bacterial culture was measured using pH meter (Thermo Scientific, Waltham, MA) at 1 h, 2 h, 4 h, 8 h, 12 h, 16 h and 24 h.

RNA-Seq

Sample preparation

S. mutans was cultured in 10 mL BHI medium until the logarithmic growth phase (OD = 0.5). The culture was centrifuged (10000 rpm, 10 min, 4 °C), then resuspended by 10 mL BHIS containing 0, 32 µg/mL (1/2MIC) and 64 µg/mL (MIC) of SH. *S. mutans* were then cultured anaerobically at 37°C for 3 h. Finally, the samples were collected, frozen in liquid nitrogen, and stored at -80°C for subsequent RNA extraction and sequencing [31,32].

RNA sequencing and data analysis

RNA sequencing (RNA-Seq) was performed by Illumina NovaSeq (Shanghai Personal Biotechnology Co., Ltd., China) [33].

A total of 1856 genes were subjected to analysis. The evaluation of differential gene expression involved the utilization of fragments per kilobase per million (FPKM) values. To examine the correlation between gene expression levels among samples, we estimated the Pearson correlation coefficient. Principal-component analysis (PCA) was employed for sample clustering within each group. Differentially expressed genes (DEGs) were defined based on specific criteria: an absolute log₂-fold change (FC) > 1 and adjusted *p* value < 0.05. DEGs were categorized as upregulated if their expression levels in 1/2 MIC SH-treated/MIC SH treated biofilm samples exceeded those in control/1/2 MIC SH treated biofilm, and vice versa. We visually represented the expression patterns of DEGs in each treatment using a volcano plot. Subsequently, functional enrichment analyses on these DEGs were conducted by utilizing KEGG annotations.

RNA extraction and quantitative real-time PCR (qPCR)

To further verify the results of RNA-Seq, we conducted qPCR to identify the gene expression levels. Sample preparation was same to biofilm formation assay. DNA extraction and purification was performed with Masterpure™ Complete DNA &RNA Purification Kit (Biosearch Technologies, USA). DNA removal and RNA reverse transcription were performed by Hifair® III 1st Strand cDNA Synthesis SuperMix for qPCR (gDNA digester plus) (Yeasen, Shanghai) to synthesize cDNAs.

The qRT-PCR analysis was performed with a LightCycler 480 system (Roche, Germany). The specific primers for the target genes are listed in Table 1. The qPCR mixture and procedure were conducted following the previously documented method [37]. Changes in gene expression were calculated with cycle threshold (CT) value based on 2^{-ΔΔCt} method [38].

Phenotypic assays of mutants

The *VicK*, *GtfB* and *GtfBC* null mutant ($\Delta vicK$, $\Delta gtfB$ and $\Delta gtfBC$), anti-sense *VicR* strain (*ASvicR*), and *OEvicK*, *OEvicR* strains were cultured in accordance with UA159. CV staining assay, colony-forming units assay and anthrone assay were conducted in accordance with the procedure mentioned above.

Cytocompatibility evaluation of SH

Human dental pulp cells (hDPCs) and human gingival fibroblasts (HGFs) were kindly provided by Dr. Zhao Li (State Key Laboratory of Oral Diseases, Sichuan University, Chengdu, China). The procedure was approved by the Hospital's Institutional Review Board at the West China Hospital of Stomatology, Sichuan University. The hDPCs and HGFs were cultured in Dulbecco's modified Eagle medium (DMEM, GIBCO, ThermoFisher Scientific, Waltham, MA, USA)/High Glucose with 10% Fetal bovine serum

Table 1. Specific primer of target genes.

Gene	Primer	Sequence (5'-3')
<i>S. mutans</i> -16S	16S-F	ATTGTTGCTCGGGCTCTCCAG
	16S-R	ATGCGGCTTGTCAGGAGTAACC
<i>S. mutans</i> - <i>VicK</i> [34]	<i>VicK</i> -F	CGGCGTGATGAATATGATGAA
	<i>VicK</i> -R	GAGGTTAATGGTGTCCGCAGT
<i>S. mutans</i> - <i>VicR</i> [35]	<i>VicR</i> -F	TGACACGATTACAGCCTTTGATG
	<i>VicR</i> -R	CGTCTAGTTCTGGTAACATTAAGTCCAATA
<i>S. mutans</i> - <i>GtfB</i> [36]	<i>GtfB</i> -F	CACTATCGGCGGTTACGAAT
	<i>GtfB</i> -R	CAATTTGGAGCAAGTCAGCA
<i>S. mutans</i> - <i>GtfC</i> [36]	<i>GtfC</i> -F	GATGCTGCAAACCTCGAACA
	<i>GtfC</i> -R	TATTGACGCTGCGTTTCTTG
<i>S. mutans</i> - <i>GtfD</i> [36]	<i>GtfD</i> -F	TTGACGGTGTTCGTGTGAT
	<i>GtfD</i> -R	AAAGCGATAGGCGCAGTTTA

(FBS, Yeasen, Shanghai) and 1% penicillin-streptomycin, in a cell incubator of 95% humidity and 5% CO₂ at 37°C.

The hDPCs and HGFs were inoculated into a 96-well plate at 10⁴ cells per well, and incubated for 24 h. SH was added in 50 mL DMEM/High Glucose with 1% penicillin-streptomycin solution for 24 h. Then, the cells were added medium with various concentrations of SH (0, 32, 64, and 128 µg/mL) and incubated for 24 h. The supernatant was detected by a Cell Counting Kit-8 (CCK-8, APExBIO Technology LLC, USA). Then, a microplate reader (Thermo Fisher, Waltham, MA, USA) was used to measure the OD at 450 nm. The cell viability rate was calculated following the criteria:

Cell viability rate (%) = $(OD_{450\text{ nm}} \text{ of control group} - OD_{450\text{ nm}} \text{ of SH treated group}) / (OD_{450\text{ nm}} \text{ of control group} - OD_{450\text{ nm}} \text{ of blank control}) \times 100\%$.

Rat caries model

The rat model was used to evaluate the anticaries effect and explore the mechanism *in vivo*. The experiment was approved by the animal research committee of West China School of Stomatology, Sichuan University (WCHSIRB-D-2022-633). 20 Specific pathogen free (SPF) Sprague-Dawley (SD) rats, aged 21 days, male, were purchased from Byrness Weil Biotech Co., Ltd. The caries model was developed according to a previous study [39]. In brief, the rats were fed with water containing 5% (wt/vol) sucrose and caries-promoting diet (Diet 2000#). From day 1 to day 3, the rats were fed with sodium ampicillin (0.1%) to inhibit oral endogenous microorganisms. Day 4 to day 6, the rats were infected with *S. mutans* (OD = 1, 0.2 mL rat/day) for 3 consecutive days. Then, divided 20 rats into 4 groups randomly: (1) double distilled water (DDW, negative control), (2) 64 µg/mL SH, (3) 128 µg/mL SH, (4) 1000 ppm NaF. Camel hairbrush was used to conduct the short-term treatment (30 s each side, once daily). After 5 weeks treatment, the rats were sacrificed and collected the dental plaque to detect the gene expression through qPCR. Then, the jaws were aseptically removed. After fixation and removed the soft tissue on the surface of the jaw, 0.4% murexide was used to stain the jaws for 12 h, and then recorded the keyes score. Micro CT (NEMO® Micro CT, PINGSENG, China) was employed to analyze the lesion depth of caries. The scanning parameters were in accordance with standard scanning of large *ex vivo* samples at medium resolution. Avater software was used to obtain the scanned images and further quantitatively analyze the lesion depth of jawbone samples.

Statistical analysis

Statistical analysis was conducted using SPSS 22.0 software (IBM Corp., Armonk, USA). After homogeneity of variance test (Levene's test) on the data, one-way ANOVA and SNK method were used for multiple comparisons between the groups. Both groups were subjected to a double-sided test, with a significance level of $\alpha = 0.05$. All figures were generated with GraphPad Prism 7 software (version 7.00 for Windows; GraphPad Prism, Inc, La Jolla, USA).

Data availability

The RNA sequencing data have been submitted to the public database Sequence Read Archive with accession number (PRJNA1131914). https://dataview.ncbi.nlm.nih.gov/object/PRJNA1131914?reviewer=bvju_posqp1ltjhqegu064t6g2f. All datasets produced and/or examined in this study can be obtained from the corresponding author upon reasonable request.

Results

SH inhibited the growth of *S. mutans*

The MIC of SH against *S. mutans* was 64 µg/mL, and the MBC of *S. mutans* was 128 µg/mL. SH significantly inhibited the growth of *S. mutans*. Briefly, after about 5 h of cultivation, the control group entered into the logarithmic phase, and the final OD_{600 nm} at 0.8, while the growth of *S. mutans* treated 32 µg/mL SH was slow and entered into the logarithmic phase at approximately 12 h with the final OD_{600 nm} at 0.6. *S. mutans* treated by 64 and 128 µg/mL SH showed no obvious growth within 24 h (Figure 1b).

SH inhibited the biofilm formation and cariogenic virulence of *S. mutans*

SH suppressed the development of biofilm in a dose dependent manner, and the inhibition rates of 32, 64 and 128 µg/mL of SH were 29.40%, 56.12% and 83.91%, respectively ($p < 0.05$) (Figure 2a). Meanwhile, SH at 32, 64 and 128 µg/mL also decreased the viable bacterial cells in the biofilms ($p < 0.05$) (Figure 2b). The SEM indicated that *S. mutans* cells in control group were densely arranged, with a smooth surface and no obvious cell lysis or cell debris. SH at different concentrations significantly reduced bacterial cells and extracellular matrix (Figure 2c). In addition, the bacterial cells in the 64 and 128 µg/mL groups showed dispersed arrangement, rough surface and distorted cell morphology (Figure 2c). CLSM showed that the biofilms from control group were dense and mainly composed of viable bacterial cells (Figure 2d,e). The biomass of biofilms treated by 32 µg/mL SH were reduced and showed more dead bacterial cells in the biofilms. The biofilms

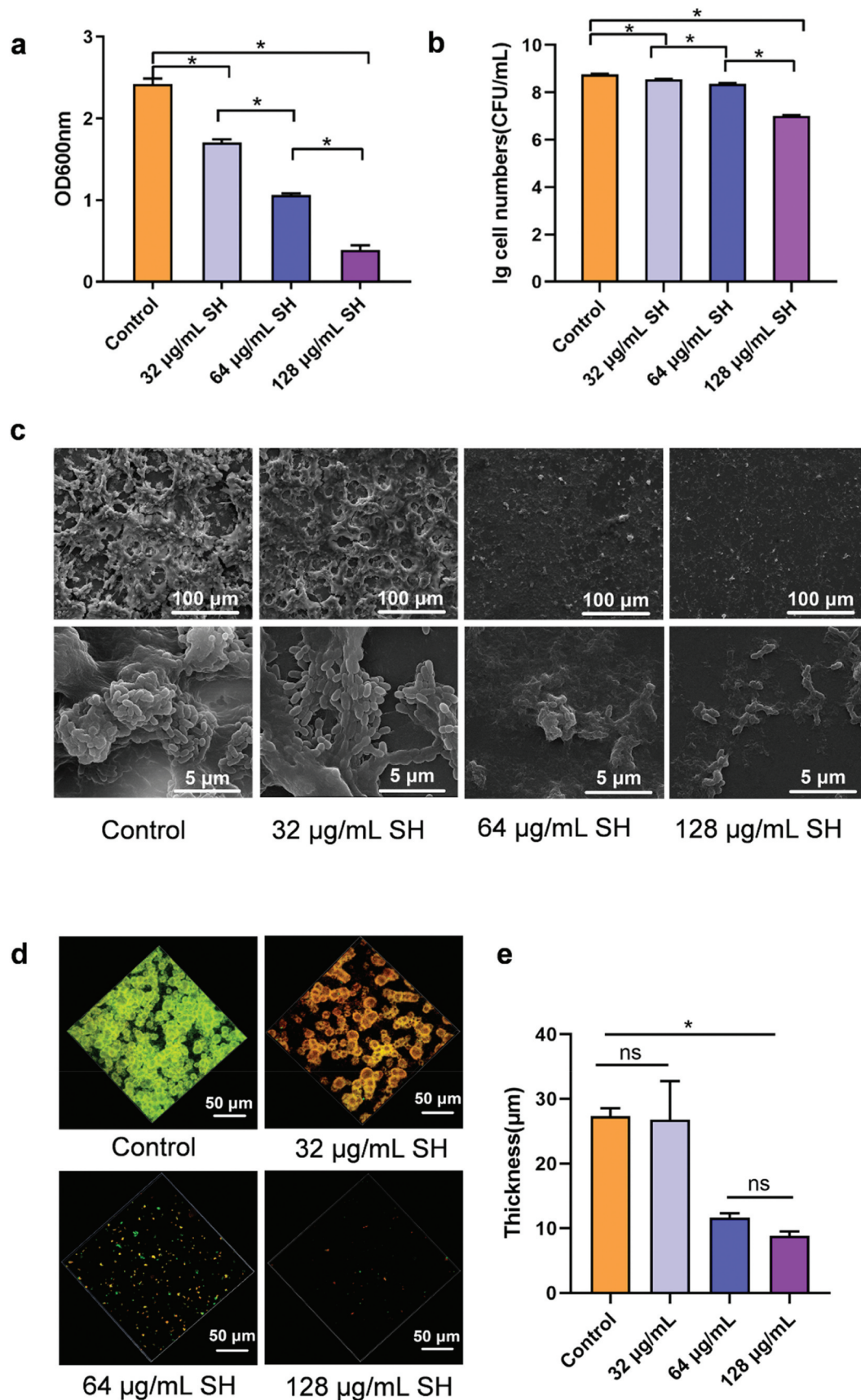


Figure 2. Effects of SH on *S. mutans* biofilm formation. (a) Biofilm biomass measured by CV staining. (b) Living cell number in *S. mutans* biofilm measured by CFU ($\lg = \log_{10}$). (c, d) Morphological changes of *S. mutans* biofilm observed by SEM (1000 \times and 20,000 \times) and CLSM (oil objective lens 60 \times). The green fluorescence is indicative of live cells, while the red fluorescence is indicative of dead cells. (e) The biofilm thickness analyzed by software NIS elements viewer 4.20. (*, $p < 0.05$; ns, not significant).

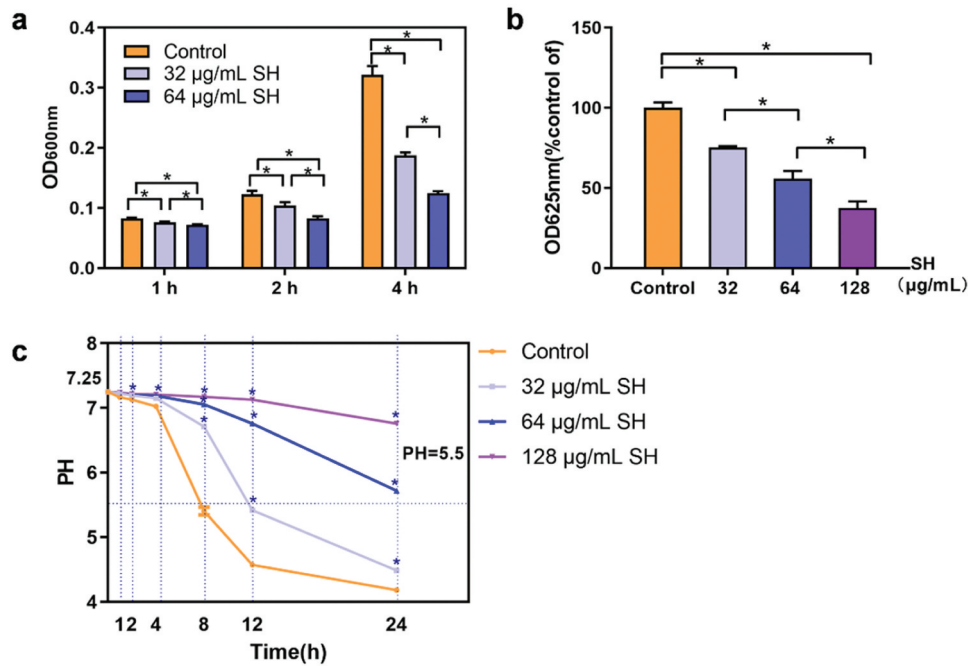


Figure 3. Effects of SH on *S. mutans* virulence factors. (a) Initial adhesion (b) Water-insoluble exopolysaccharides measured by anthrone assay (c) Acid production (*, $p < 0.05$; ns, not significant).

treated by 64 and 128 µg/mL of SH became loose and thin, and the proportions of dead cells were significantly increased (Figure 2d,e)

SH significantly inhibited the initial adhesion of *S. mutans* (Figure 3a). At 1 h, the inhibition rates of 32 and 64 µg/mL of SH were 7.6% and 12.9%, and were 15.7% and 32.8% at 2 h, while at 4 h, the rates were become 41.8% and 61.2%, respectively (Figure 3a). Extracellular insoluble polysaccharides were reduced 24.7%, 44.1% and 62.5% by 32, 64 and 128 µg/mL of SH, respectively (Figure 3b). While SH also significantly reduced the acid production of *S. mutans* by 32, 64 and 128 µg/mL of SH (Figure 3c). Especially, the pH of the culture treated by 64 µg/mL SH was 5.71 at 24 h which was higher than the clinical pH threshold for enamel demineralization (pH = 5.5) (Figure 3c), while there was no significant decrease of pH value treated by 128 µg/mL SH within 24 h (Figure 3c).

SH downregulated the VicRK pathway of *S. mutans*

The transcriptome of *S. mutans* were sequenced to investigate the possible mechanisms of SH against *S. mutans*. PCA results showed that there were significant differences in gene expression patterns of *S. mutans* after the treatment with different concentrations of SH (Figure S1). Compared to the control group, the 32 µg/mL group exhibited 217 differentially expressed genes (DEGs) with 133 upregulated genes and 84 downregulated genes (Figure 4a). The 64 µg/mL group exhibited 505 DEGs with 269

upregulated genes and 236 downregulated genes (Figure 4b). KEGG enrichment pathway analysis of DEGs showed that when treated by both 32 and 64 µg/mL of SH, the two-component system were significantly enriched (Figure 4c,d), in which the VicRK system was one of the most downregulated pathways (Figure 4e, Table S1). The VicRK system regulated genes related to the EPS synthesis, cell wall biosynthesis, cell division, and bacteriocin production and autolysin were listed in Table S2, and only the genes related to EPS production and biofilm formation were downregulated (Figure 4f). The qPCR assay also confirmed that both 32 and 64 µg/mL SH significantly downregulated the expressions of *VicK*, *VicR*, *GtfC* and *GtfD* (Figure 4g and Figure S2). These results were in line with the actions of SH on *S. mutans* biofilm formation and EPS production, indicating that SH could inhibit the VicRK system to downregulate the EPS production and then reduce the biofilm formation and cariogenicity.

SH interfered the biofilm formation and EPS generation of mutants from VicRK pathway

Since SH was able to inhibit the expressions of genes from VicRK system and related EPS biosynthesis, $\Delta vicK$, $\Delta vicR$, $\Delta vicK$ and $\Delta vicR$ strains were then employed to validate the inhibitory actions of SH on VicRK system, while $\Delta gtfB$ and $\Delta gtfBC$ were also involved as EPS defect controls to evaluate the inhibition of SH on EPS production. Compared with WT strain, the biofilm biomass, viable cells in biofilms and EPS production from $\Delta vicK$ and $\Delta vicR$

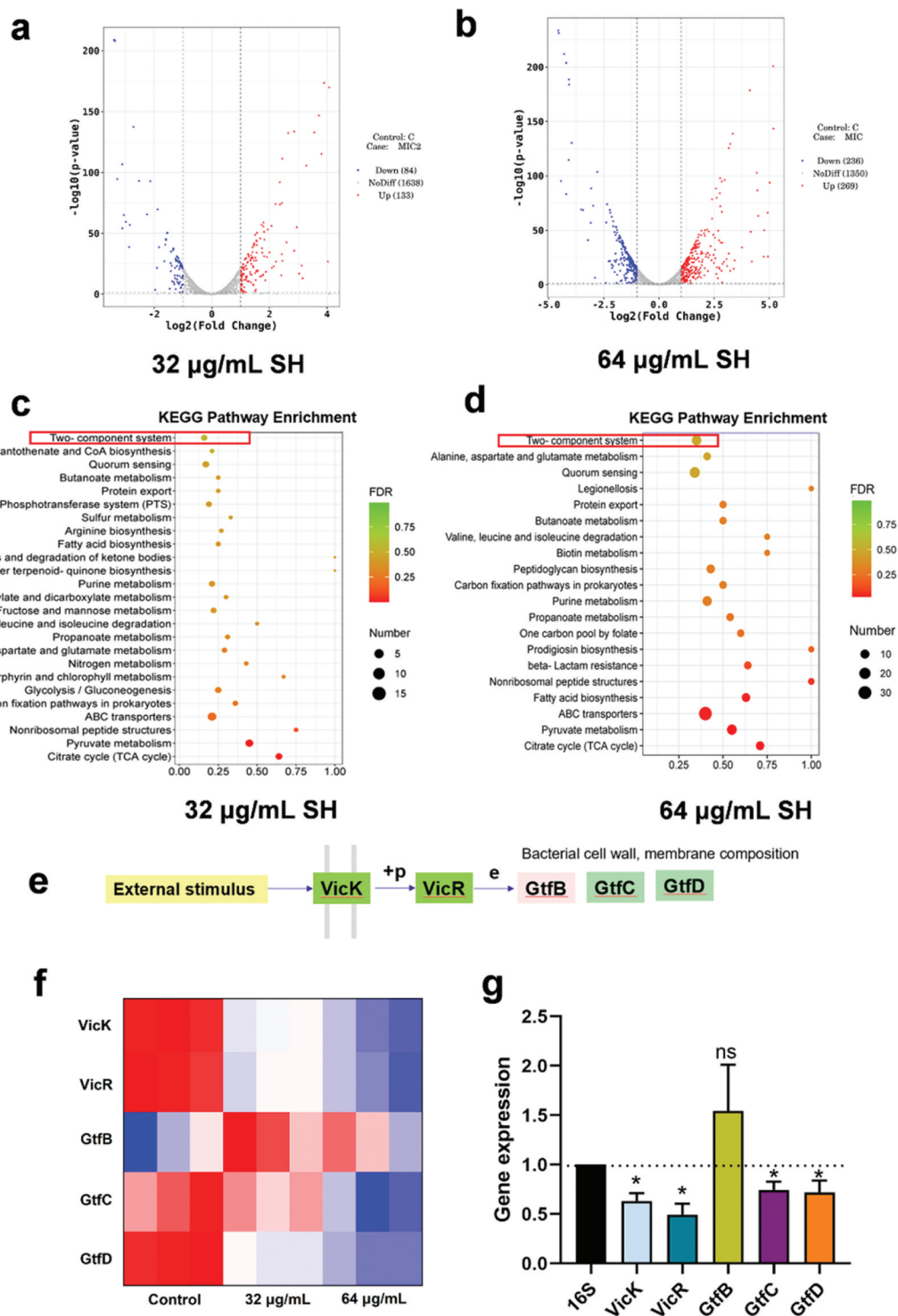


Figure 4. SH downregulated the VicRK pathway of *S. mutans*. (a, b) Volcano plot of centered and scaled FPKM values of DEGs indicating significant expression changes under SH treated. (c, d) KEGG pathway enrichment analysis indicating that the two-component system was the DEG-enriched pathway. (e) Scheme of VicRK pathway. (f) Heatmap analysis on genes expressions of the VicRK system. (g) The differential expression of VicRK pathway related genes under the 64 µg/mL treatment, including *VicK*, *VicR*, *GtfB*, *GtfC* and *GtfD*, verified by qPCR (*, $p < 0.05$; ns, not significant).

mutants were significantly reduced after SH treatment, and the decreased proportion was larger than that from the WT ($p < 0.05$) (Figure 5a-c). Similarly, $\Delta gtfB$ and $\Delta gtfBC$ treated by SH also showed a significant reduction in biofilm biomass, viable cells in biofilms, and EPS productions, compared

with WT strain ($p < 0.05$) (Figure 5d-f). These results indicated that $\Delta vicK$, $\Delta gtfB$, $\Delta gtfBC$, $\Delta vicR$ showed higher sensitivity to SH.

OEvicK and *OEvicR* strains were then employed to evaluate whether the overexpression of *VicK* and *VicR* could reduce the activities of SH. SH slightly

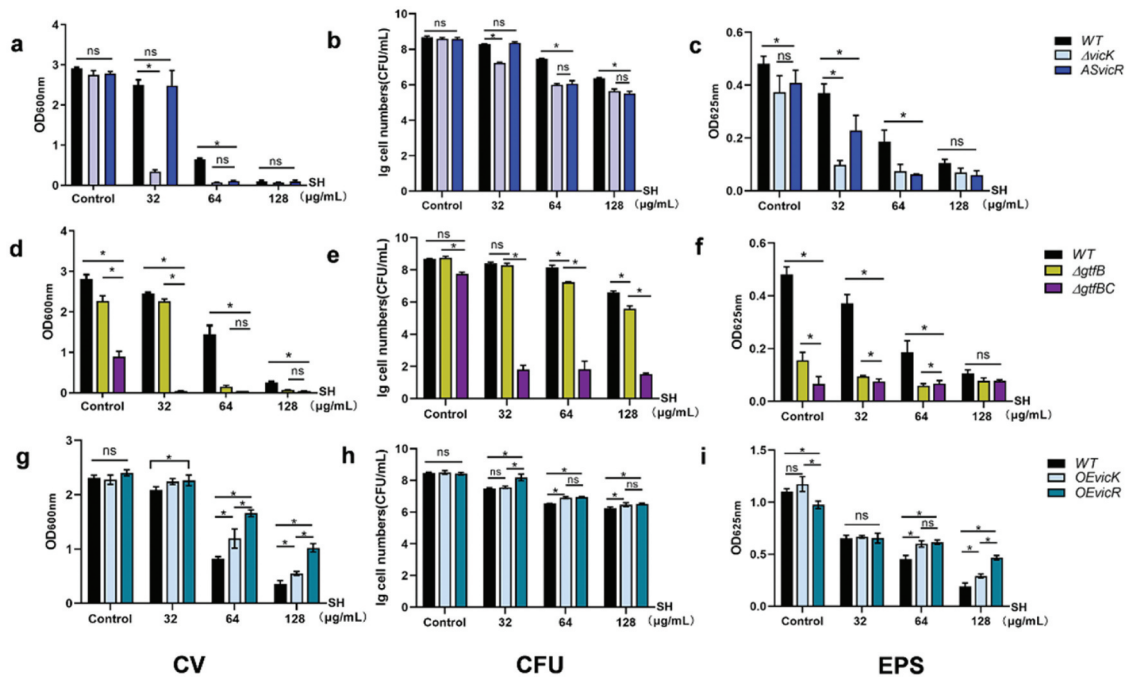


Figure 5. The mutants from the *VicRK* pathway interfered with the activities of SH. (a,b,c) the biofilm biomass (a), biofilm viable bacteria (b), and EPS production (c) of *ΔvicK* and *ASvicR* compared with wild type strain. (d, e, f) the biofilm biomass (d), viable bacterial cells in biofilm (e), and EPS production (f) of *ΔgtfB* and *ΔgtfBC* compared with wild type strain. (g, h, i) the biofilm biomass (g), biofilm viable bacteria (h), and EPS production (i) of *OEvicK* and *OEvicR* compared with wild type. (*, $p < 0.05$; ns, not significant).

decreased the EPS productions of *OEvicK* and *OEvicR*, and showed no significant effects on the biofilm biomass and viable bacterial cells from the biofilms (Figure 5g-i). Meanwhile, after the treatment of SH, the biofilm biomass, viable bacteria cells, and EPS production of *OEvicK* and *OEvicR* were higher than WT ($p < 0.05$) (Figure 5g-i), indicating that *OEvicK* and *OEvicR* showed lower sensitivity to SH treatment.

SH downregulated the *VicRK* pathway of *S. mutans* from the dental plaques of rats

The expressions of *VicK* and *VicR* of *S. mutans* from the dental plaques of rats showed a dose-dependent decrease when the rats were treated by both 64 and 128 µg/mL SH ($p < 0.05$), while NaF did not affect their expressions (Figure 6a,b). The expressions of *GtfB*, *GtfC*, *GtfD* were inhibited by 64 and 128 µg/mL SH and NaF ($p < 0.05$) (Figure 6c-e).

SH showed good anti-carries effect in vivo

Keyes score

Both 64 and 128 µg/mL of SH showed significant inhibitory effects on sulcal caries and smooth surface caries ($p < 0.05$).

Smooth surface caries. 64 and 128 µg/mL of SH effectively inhibited the occurrence of enamel and slightly dental caries ($p < 0.05$), and 128 µg/mL of

SH had no significant difference with 1000 ppm NaF ($p > 0.05$) (Figure 7a,c). No moderate or extensive dental caries were detected when treated by both SH and NaF (Figure 7a,c).

Sulcal caries. 64 and 128 µg/mL of SH effectively inhibited the occurrence of enamel caries ($p < 0.05$), but showed inferior effects compared to 1000 ppm NaF ($p < 0.05$) (Figure 7b,d). 64 and 128 µg/mL of SH also inhibited slightly and moderate dental caries, while 128 µg/mL of SH showed no significant difference with 1000 ppm NaF ($p > 0.05$) (Figure 7b,d). No extensive dental caries was detected when treated by both SH and NaF (Figure 7b,d).

Micro CT

Compared with the DDW group, 64 and 128 µg/mL of SH effectively inhibited the occurrence and development of dental caries as the dental caries lesion depths were significantly reduced ($p < 0.05$), while the 128 µg/mL of SH showed no significant difference with 1000 ppm NaF ($p > 0.05$) (Figure 7e,f), indicating the prevention abilities of SH on the progression of dental caries.

SH showed good biocompatibility on host cells and rats

The human dental pulp cells (hDPCs) and human gingival fibroblasts (HGFs) were involved to test the cytotoxicity of SH. The 32, 64 and 128 µg/mL of SH

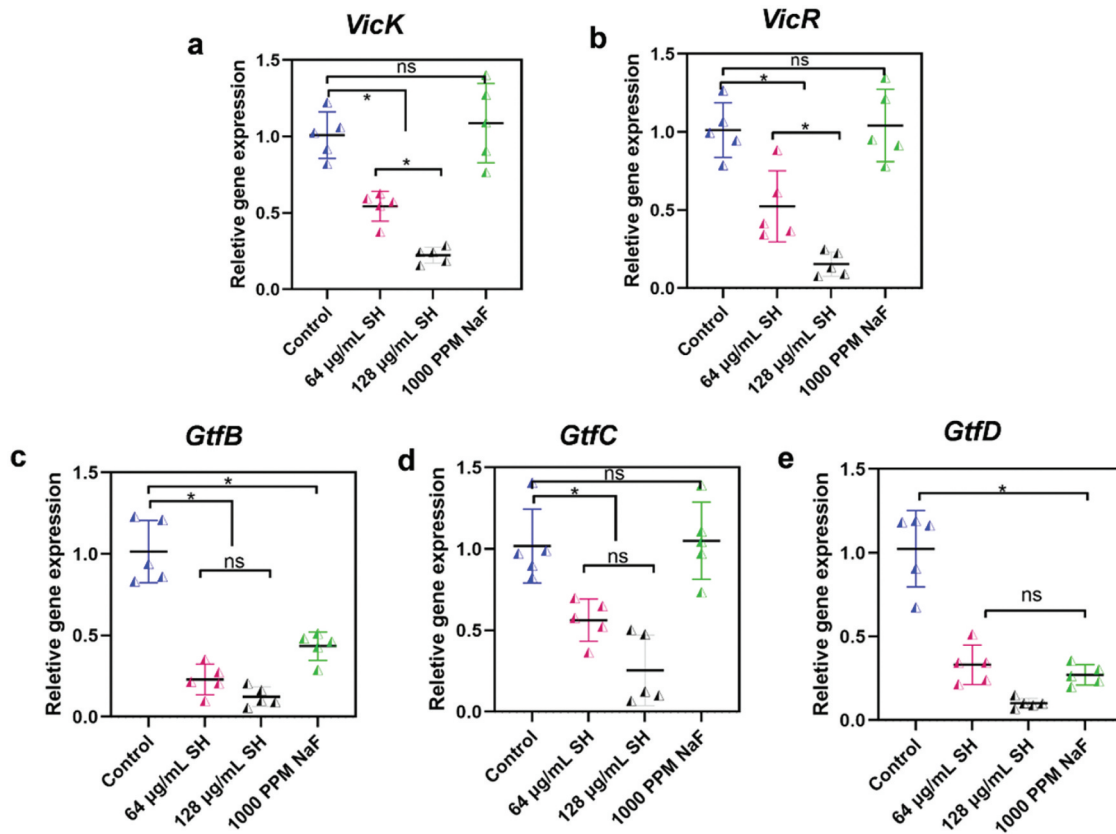


Figure 6. Gene expressions of *VicK*, *VicR* and EPS production related *GtfB*, *GtfC* and *GtfD* from the dental plaques. The differential expressions of the VicRK pathway related genes: *VicK*, *VicR*, *GtfB*, *GtfC* and *GtfD* were confirmed from the rat dental plaques through qPCR with 16S rRNA as the internal control (*, $p < 0.05$; ns, not significant).

showed no cytotoxicity on the viability of both hDPCs and HGFs (Figure 8a,b) ($p > 0.05$), indicating the good biocompatibility on host cells.

When the rats were treated by SH, their weights showed no significant difference with the ones treated by water (Figure 8c), while there were also no pathological changes in the structure and cellular morphology on liver (Figure 8d), kidney (Figure 8e) and heart (Figure 8f), indicating that SH showed no systematic toxicity in rats.

Discussion

The high incidence of caries is a great challenge to public health and exacerbates the socio-economic burden [2,3]. However, the current preventive options, such as fluoride, are insufficient to meet the need of clinical practice, which poses the urgent necessity for the development of new anticaries strategies [7,10]. Natural products have great potential to be the practical alternative for antibiotics in infectious diseases due to their diverse functionalities and cost-effectiveness [14,15].

SH has been proved its antibacterial and anti-fungi effects in recent studies. In this study, we revealed that SH suppressed *S. mutans* growth and inhibited its biofilm formation and cariogenic virulence factors

in a dose-dependent manner. We found that 32 µg/mL of SH could reduce the planktonic growth of *S. mutans*, while the MIC (64 µg/mL) and the MBC (128 µg/mL) of SH completely inhibited *S. mutans* planktonic growth. Therefore, to reveal the anti-*S. mutans* mechanisms of SH, 1/2MIC (32 µg/mL) and MIC (64 µg/mL) of SH treated *S. mutans* cells were chosen for RNA-seq as these concentrations could accumulate enough biomass for RNA extraction and sequencing compared to that the MBC at 128 µg/mL killed most bacterial cells. However, 128 µg/mL of SH showed strong biofilm and cariogenic virulence inhibitions, so this concentration was also employed to combat the dental caries formation in rat models. As expected, 128 µg/mL of SH significantly inhibited the development of dental caries even comparable with 1000 ppm NaF and showed well biocompatibility on host cells and rats. RNA-seq analysis showed that *VicRK* two-component system, a pathway closely related to biofilm formation and EPS production, was significantly downregulated. The *VicRKX* signal transduction system is composed of three encoding proteins: *VicK*, a histidine protein kinase; *VicR*, a global response regulator (RR); and *VicX*, a putative hydrolase [24,27,40]. *VicK* plays an essential role in detecting and transmitting chemical signals from the environment to downstream

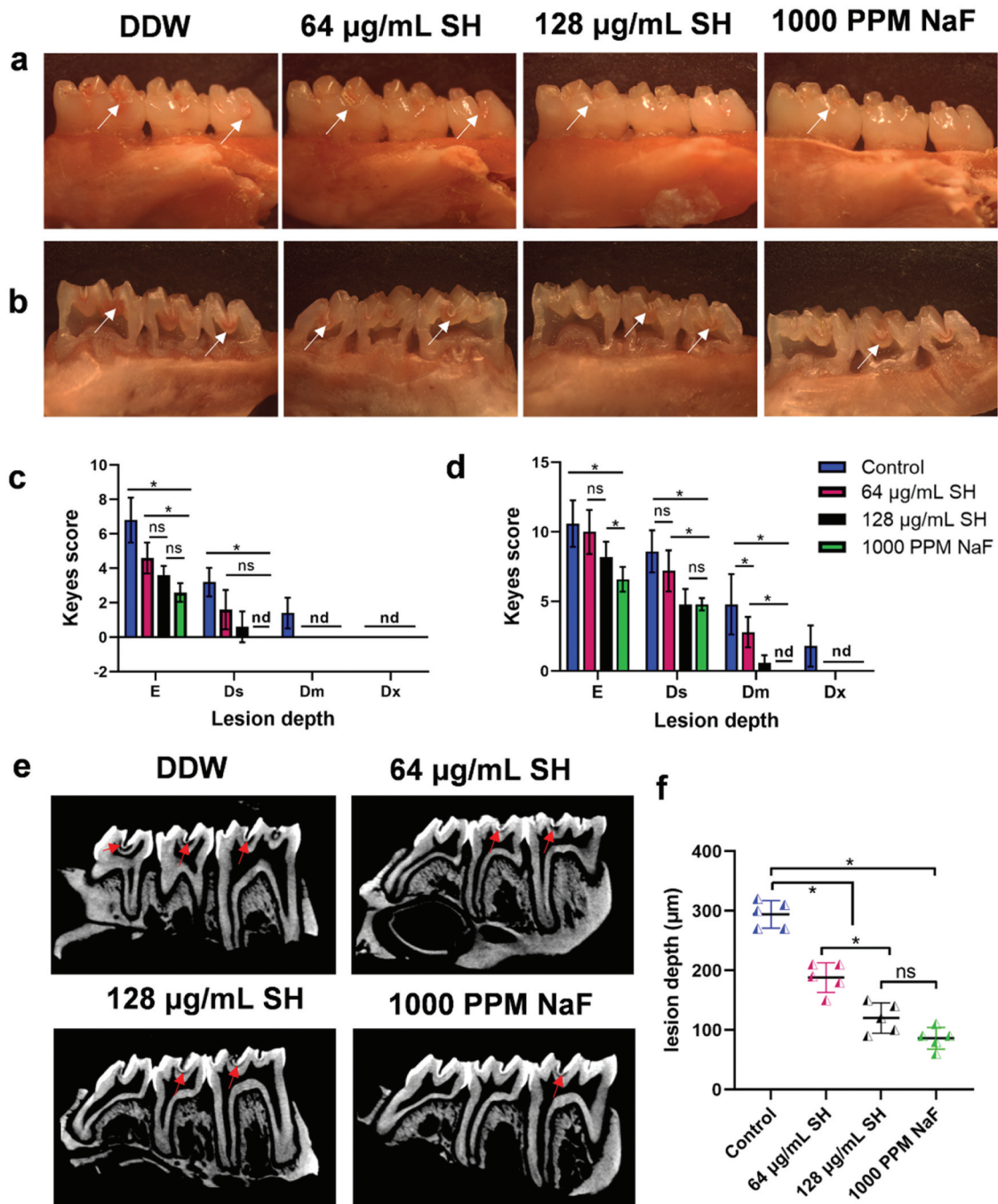


Figure 7. Anti-carries effect of SH treatment *in vivo*. (a, b) Staining images of smooth surface caries and sulcal caries in rat mandibular samples. (c) Keyes score of smooth surface caries. (d) Keyes score of sulcal caries. (e) Micro CT images of rat mandibular samples. (f) The maximum lesion depth of rat teeth. (*, $p < 0.05$; ns, not significant).

regulatory proteins such as VicR and GcrR [41]. VicR could then regulate the biofilm formation related genes like *GtfB/C*, *Ftf* and *GbpB* [31,42]. Deng *et al.* found that VicK null mutant showed less biofilm formation and EPS production, and *GtfD*, *Ftf* and *GbpB* were downregulated and *GtfB* was upregulated [24]. Lei *et al.* found that ASvicR, an antisense VicR RNA associated with RNase III-encoding (*rnc*) gene, could regulate VicR activity, downregulated *GtfBCD* and *Ftf*, and the overexpression VicR antisense RNA significantly impaired bacterial growth, biofilm formation, and finally reduced cariogenicity *in vivo*

[27,41]. In our study, we found that SH could down-regulate the expressions of *VicK* and *VicR* genes and then inhibited the expressions of *GtfB*, *GtfC* and *GtfD*. When compared to WT, $\Delta vicK$, $\Delta SvicR$, $\Delta gtfB$ and $\Delta gtfBC$ were more sensitive to SH, while *OEvicK* and *OEvicR* strains were more resistant, furtherly indicating the inhibitory actions of SH on *VicRK* two-component system.

According to the transcriptome analysis, phospho-transferase system (PTS) was also significantly down-regulated, especially the mannose-phosphotransferase system. The sugar PTS is the major sugar uptake

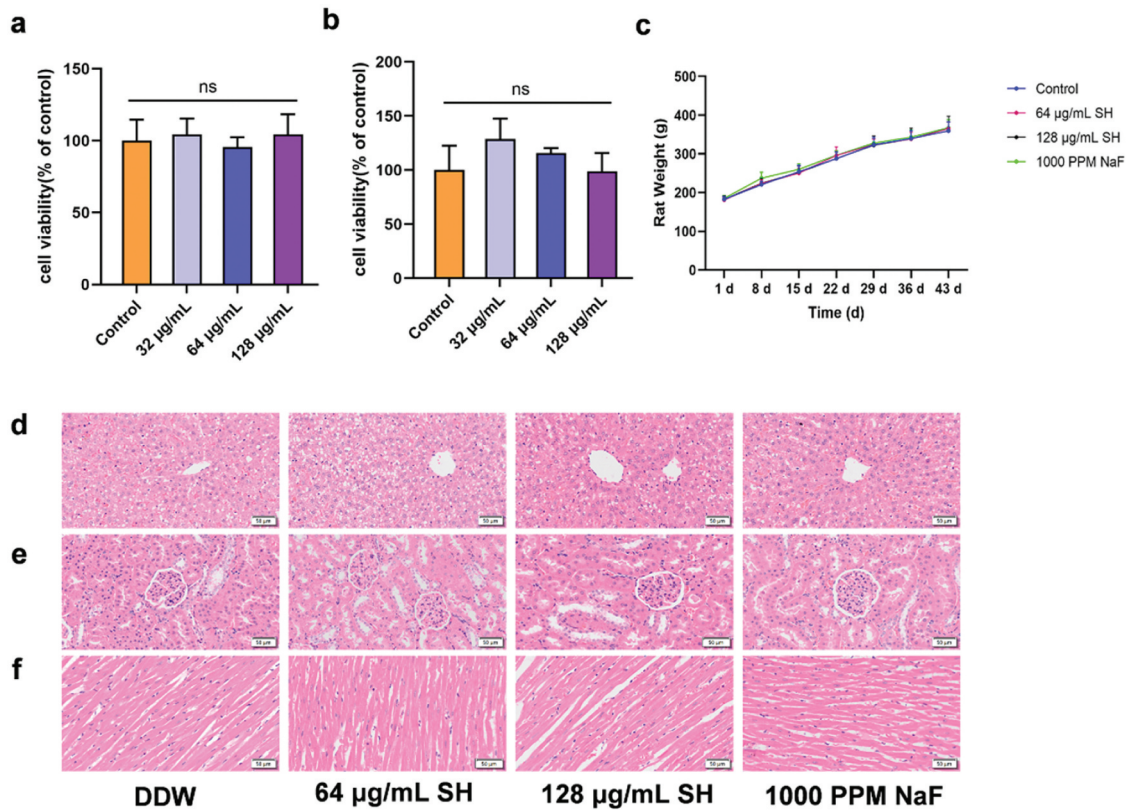


Figure 8. Biocompatibility of SH on host cells and rats. (a, b) the cytotoxicity and proliferation of hDPCs (a) and HGFs (b) under SH treatment. (c) The weight of rats. (d) HE staining of rats liver. (e) HE staining of rats kidney. (f) HE staining of rats heart.

system in oral streptococci [43]. The water-soluble glucans and water-insoluble glucans of *S. mutans* are mainly composed of mannose and glucose [24]. Hence, in addition to the VicRK, the downregulation of PTS system by SH may also contribute to its inhibitory activities on *S. mutans* EPS productions. Fatty acid biosynthesis, which is associated with acid tolerance [44], also significantly inhibited after SH treatment, but the mechanisms need to be further investigated.

The antibacterial mechanisms of SH have been investigated in different species. Ye *et al.* found that SH inhibited the growth of *Bacillus subtilis* by inserting into the phospholipid bilayer and influencing membrane fluidity, which was closely related to the hydrophobic interaction between SH and membrane proteins [45]. Wang *et al.* reported that SH reduced *Pseudomonas aeruginosa* biofilm formation and inhibited the gene expression of *BdlA* (a key gene regulating the dispersion reaction) to regulate the dispersion of biofilm [46]. Wu *et al.* found that SH suppressed the production of N-acyl homoserine lactone (AHL), a quorum sensing signaling molecule, by reducing the expression of *LasI* in *Pseudomonas aeruginosa*. Meanwhile, SH down-regulated the gene expression of *LasR*, an AHL sensor and transcriptional regulator, and inhibited the quorum sensing-related virulence factors, including pyocyanin and *LasA* [47]. In this study, we found that SH inhibited

the VicRK system to regulate the EPS production in *S. mutans*. The different actions of SH indicated that SH may have different targets in different bacterial species.

Fluoride is widely recommended as anti-caries compound and 1000 ppm NaF was usually used into mouthwash for controlling dental caries [48], and was also commonly used as a positive control group in rat caries model [49]. However, there are many limitations of fluoride. Fluoride cannot inhibit continuous biofilm development and could lead to the changes in oral and gut microbiota [50]. Some fluoride resistant bacterial species have been isolated from oral cavities [51]. Furthermore, the excessive ingestion of fluoride may cause toxic and harmful effects for the human body, such as fluorosis [52]. While SH showed better antibiofilm effects on different species, including fungal species, such as *Candida albicans* [53]. SH also showed the potential in maintaining microflora stability and anti-inflammation [54], which improves its possibility of clinical usage. Moreover, even much higher dosage of SH in rat intestinal malfunction treatment showed no significant side-effect [55]. The dental caries rat models from our results showed that different concentrations of SH could inhibit the occurrence and development of dental caries, especially the anti-caries capabilities of 128 µg/mL SH and 1000 ppm NaF were comparable. The well biocompatibility of this concentration

of SH on host cells and rats furtherly indicated that 128 µg/mL SH could be a practical dosage for further anti-carries applications.

The decrease expressions of *VicK*, *VicR*, *GtfC* and *GtfD* from the rat dental plaques treated by SH suggested that SH could inhibit dental caries through VicRK pathway. VicRK could regulate the sucrose metabolism and biofilm formation in *S. mutans* [24]. Its homologues have been found in other *Staphylococci* [56] and *Streptococci* [57], and this pathway has been developed as novel targets to combat antibiotic resistance. Zhang *et al.* designed multi-targeted antisense nucleotide sequences against VicK to inhibit biofilm formation and virulence of *S. mutans* [58]. Liu *et al.* identified a compound (a 2-aminoimidazole derivative) that inhibited biofilm formation of *Staphylococcus aureus* and *S. mutans*. This compound could bind to *S. mutans* VicR to inhibit the expression of *VicR* and *VicR*-regulated genes, including Gtfs, and attenuated virulence of *S. mutans* in a dental caries rat model [59]. While in our study, we also found that SH could down-regulate VicRK to inhibit the cariogenicity of *S. mutans*.

In conclusion, SH repressed the VicKR system of *S. mutans* to inhibit the cariogenic virulence factors and the development of dental caries. This study provided a promising therapeutic strategy for clinical prevention and treatment of oral caries and highlighted that VicRK system was a practical target for the development of anti-carries agents.

Disclosure statement

No potential conflict of interest was reported by the author(s).

Funding

This work was supported by grants from the National Natural Science Foundation of China [Grant No.82071111], Key Research and Development Projects of the Science and Technology Department of Sichuan Province [2024YFHZ0042], Natural Science Foundation of Sichuan province [2024NSFSC0546] and Health Commission of Sichuan Province [chuanganyan 2024-901].

CRedit authorship contribution statement

Yaqi Chi: Methodology, Investigation, Formal analysis, Writing the original draft. Ye Wang: Investigation. Di Fu: Investigation. Lin Yao: Investigation. Mingying Wei: Investigation. Ge Zhou: Investigation. Ling Zou: Resources, Funding acquisition, Project administration. Biao Ren: Validation, Formal analysis, Conceptualization, Writing-review and editing, Supervision.

ORCID

Ling Zou  <http://orcid.org/0000-0002-6022-2911>

References

- [1] Selwitz RH, Ismail AI, Pitts NB. Dental caries. *Lancet*. 2007;369(9555):51–59. doi: 10.1016/S0140-6736(07)60031-2
- [2] Bernabe E, Marcenes W, Hernandez CR, et al. Global, regional, and national levels and trends in burden of oral conditions from 1990 to 2017: a systematic analysis for the global burden of disease 2017 study. *J Dent Res*. 2020;99(4):362–373. doi: 10.1177/0022034520908533
- [3] Jain N, Dutt U, Radenkov I, et al. WHO's global oral health status report 2022: actions, discussion and implementation. *Oral Dis*. 2024;30(2):73–79. doi: 10.1111/odi.14516
- [4] Lamont RJ, Koo H, Hajishengallis G. The oral microbiota: dynamic communities and host interactions. *Nat Rev Microbiol*. 2018;16(12):745–759. doi: 10.1038/s41579-018-0089-x
- [5] Garcia SS, Blackledge MS, Michalek S, et al. Targeting of *Streptococcus mutans* biofilms by a novel small molecule prevents dental caries and preserves the oral microbiome. *J Dent Res*. 2017;96(7):807–814. doi: 10.1177/0022034517698096
- [6] Ciofu O, Rojo-Moliner E, Macià MD, et al. Antibiotic treatment of biofilm infections. *APMIS*. 2017;125(4):304–319. doi: 10.1111/apm.12673
- [7] Koo H, Allan RN, Howlin RP, et al. Targeting microbial biofilms: current and prospective therapeutic strategies. *Nat Rev Microbiol*. 2017;15(12):740–755. doi: 10.1038/nrmicro.2017.99
- [8] Thurnheer T, Belibasakis GN. Effect of sodium fluoride on oral biofilm microbiota and enamel demineralization. *Arch Oral Biol*. 2018;89:77–83. doi: 10.1016/j.archoralbio.2018.02.010
- [9] Featherstone JD. Prevention and reversal of dental caries: role of low level fluoride. *Comm Dent Oral Epid*. 1999;27(1):31–40. doi: 10.1111/j.1600-0528.1999.tb01989.x
- [10] Huang Y, Liu Y, Pandey NK, et al. Iron oxide nanozymes stabilize stannous fluoride for targeted biofilm killing and synergistic oral disease prevention. *Nat Commun*. 2023;14(1):6087. doi: 10.1038/s41467-023-41687-8
- [11] Marquis RE. Antimicrobial actions of fluoride for oral bacteria. *Can J Microbiol*. 1995;41(11):955–964. doi: 10.1139/m95-133
- [12] Hicks J, Garcia-Godoy F, Flaitz C. Biological factors in dental caries: role of saliva and dental plaque in the dynamic process of demineralization and remineralization (part 1). *J Clin Pediatr Dent*. 2003;28(1):47–52. doi: 10.17796/jcpd.28.1.yg6m443046k50u20
- [13] Tse BN, Adalja AA, Houchens C, et al. Challenges and opportunities of nontraditional approaches to treating bacterial infections. *Clin Infect Dis*. 2017;65(3):495–500. doi: 10.1093/cid/cix320
- [14] Melander RJ, Basak AK, Melander C. Natural products as inspiration for the development of bacterial antibiofilm agents. *Nat Prod Rep*. 2020;37(11):1454–1477. doi: 10.1039/D0NP00022A
- [15] Chi Y, Wang Y, Ji M, et al. Natural products from traditional medicine as promising agents targeting at

- different stages of oral biofilm development. *Front Microbiol.* **2022**;13:955459. doi: [10.3389/fmicb.2022.955459](https://doi.org/10.3389/fmicb.2022.955459)
- [16] Shao J, Cheng H, Wang C, et al. A phytoanticipin derivative, sodium houttuynfonate, induces in vitro synergistic effects with levofloxacin against biofilm formation by *Pseudomonas aeruginosa*. *Molecules.* **2012**;17(9):11242–11254. doi: [10.3390/molecules170911242](https://doi.org/10.3390/molecules170911242)
- [17] Zhao Y, Mei L, Si Y, et al. Sodium new houttuynfonate affects transcriptome and virulence factors of *Pseudomonas aeruginosa* controlled by quorum sensing. *Front Pharmacol.* **2020**;11:572375. doi: [10.3389/fphar.2020.572375](https://doi.org/10.3389/fphar.2020.572375)
- [18] Shingnaisui K, Dey T, Manna P, et al. Therapeutic potentials of *Houttuynia cordata* thunb. against inflammation and oxidative stress: a review. *J Ethnopharmacol.* **2018**;220:35–43. doi: [10.1016/j.jep.2018.03.038](https://doi.org/10.1016/j.jep.2018.03.038)
- [19] Lu HM, Liang YZ, Yi LZ, et al. Anti-inflammatory effect of *Houttuynia cordata* injection. *J Ethnopharmacol.* **2006**;104(1–2):245–249. doi: [10.1016/j.jep.2005.09.012](https://doi.org/10.1016/j.jep.2005.09.012)
- [20] Liu X, Zhong L, Xie J, et al. Sodium houttuynfonate: a review of its antimicrobial, anti-inflammatory and cardiovascular protective effects. *Eur J Pharmacol.* **2021**;902:174110. doi: [10.1016/j.ejphar.2021.174110](https://doi.org/10.1016/j.ejphar.2021.174110)
- [21] Ye X, Li X, Yuan L, et al. Interaction of houttuynfonate homologues with the cell membrane of gram-positive and gram-negative bacteria. *Colloids Surfaces A: Physicochem Eng Aspects.* **2007**;301(1):412–418. doi: [10.1016/j.colsurfa.2007.01.012](https://doi.org/10.1016/j.colsurfa.2007.01.012)
- [22] Shao J, Cheng H, Wang C, et al. Sodium houttuynfonate, a potential phytoanticipin derivative of antibacterial agent, inhibits bacterial attachment and pyocyanine secretion of *Pseudomonas aeruginosa* by attenuating flagella-mediated swimming motility. *World J Microbiol Biotechnol.* **2013**;29(12):2373–2378.
- [23] Wang TQ, Chen XF, Li L, et al. Characterization of nucleotides and nucleotide sugars in *Candida albicans* by high performance liquid chromatography–mass spectrometry with a porous graphite carbon column. *Analytical Lett.* **2014**;47(2):234–249. doi: [10.1080/00032719.2013.836657](https://doi.org/10.1080/00032719.2013.836657)
- [24] Deng Y, Yang Y, Zhang B, et al. The vicK gene of *Streptococcus mutans* mediates its cariogenicity via exopolysaccharides metabolism. *Int J Oral Sci.* **2021**;13(1):45. doi: [10.1038/s41368-021-00149-x](https://doi.org/10.1038/s41368-021-00149-x)
- [25] Liu Y, Wang Z, Zhou Z, et al. *Candida albicans* CHK1 gene regulates its cross-kingdom interactions with *Streptococcus mutans* to promote caries. *Appl Microbiol Biotechnol.* **2022**;106(21):7251–7263. doi: [10.1007/s00253-022-12211-7](https://doi.org/10.1007/s00253-022-12211-7)
- [26] Ren Z, Cui T, Zeng J, et al. Molecule targeting glucosyltransferase inhibits *Streptococcus mutans* biofilm formation and virulence. *Antimicrob Agents Chemother.* **2016**;60(1):126–135. doi: [10.1128/AAC.00919-15](https://doi.org/10.1128/AAC.00919-15)
- [27] Lei L, Stipp RN, Chen T, et al. Activity of *Streptococcus mutans* VicR is modulated by antisense RNA. *J Dent Res.* **2018**;97(13):1477–1484. doi: [10.1177/0022034518781765](https://doi.org/10.1177/0022034518781765)
- [28] Yan J, Gong T, Ma Q, et al. vicR overexpression in *Streptococcus mutans* causes aggregation and affects interspecies competition. *Mol Oral Microbiol.* **2023**;38(3):224–236. doi: [10.1111/omi.12407](https://doi.org/10.1111/omi.12407)
- [29] Deng L, Li W, He Y, et al. Cross-kingdom interaction of *Candida albicans* and *Actinomyces viscosus* elevated cariogenic virulence. *Arch Oral Biol.* **2019**;100:106–112. doi: [10.1016/j.archoralbio.2019.02.008](https://doi.org/10.1016/j.archoralbio.2019.02.008)
- [30] Wang Y, Wang X, Jiang W, et al. Antimicrobial peptide GH12 suppresses cariogenic virulence factors of *Streptococcus mutans*. *J Oral Microbiol.* **2018**;10(1):1442089. doi: [10.1080/20002297.2018.1442089](https://doi.org/10.1080/20002297.2018.1442089)
- [31] Senadheera DB, Cordova M, Ayala EA, et al. Regulation of bacteriocin production and cell death by the VicRK signaling system in *Streptococcus mutans*. *J Bacteriol.* **2012**;194(6):1307–1316. doi: [10.1128/JB.06071-11](https://doi.org/10.1128/JB.06071-11)
- [32] Khemiri I, Tebbji F, Sellam A. Transcriptome analysis uncovers a link between copper metabolism, and both fungal fitness and antifungal sensitivity in the opportunistic yeast *Candida albicans*. *Front Microbiol.* **2020**;11:935. doi: [10.3389/fmicb.2020.00935](https://doi.org/10.3389/fmicb.2020.00935)
- [33] Xiong K, Zhu H, Li Y, et al. The arginine biosynthesis pathway of *Candida albicans* regulates its cross-kingdom interaction with *Actinomyces viscosus* to promote root caries. *Microbiol Spectr.* **2022**;10(4):e0078222. doi: [10.1128/spectrum.00782-22](https://doi.org/10.1128/spectrum.00782-22)
- [34] Alves LA, Ganguly T, Harth-Chú ÉN, et al. PepO is a target of the two-component systems VicRK and CovR required for systemic virulence of *Streptococcus mutans*. *Virulence.* **2020**;11(1):521–536.
- [35] He Z, Huang Z, Jiang W, et al. Antimicrobial activity of cinnamaldehyde on *Streptococcus mutans* biofilms. *Front Microbiol.* **2019**;10:2241.
- [36] Li MY, Huang RJ, Zhou XD, et al. Role of sortase in *Streptococcus mutans* under the effect of nicotine. *Int J Oral Sci.* **2013**;5(4):206–211. doi: [10.1038/ijos.2013.86](https://doi.org/10.1038/ijos.2013.86)
- [37] Xu X, Zhou XD, Wu CD. The tea catechin epigallocatechin gallate suppresses cariogenic virulence factors of *Streptococcus mutans*. *Antimicrob Agents Chemother.* **2011**;55(3):1229–1236. doi: [10.1128/AAC.01016-10](https://doi.org/10.1128/AAC.01016-10)
- [38] Pfaffl MW. A new mathematical model for relative quantification in real-time RT-PCR. *Nucleic Acids Res.* **2001**;29(9):45e–45. doi: [10.1093/nar/29.9.e45](https://doi.org/10.1093/nar/29.9.e45)
- [39] Jiang W, Wang Y, Luo J, et al. Antimicrobial peptide GH12 prevents dental caries by regulating dental plaque microbiota. *Appl Environ Microbiol.* **2020**;86(14):e00527–20. doi: [10.1128/AEM.00527-20](https://doi.org/10.1128/AEM.00527-20)
- [40] Wagner C, Saizieu AD, Schönfeld H-J, et al. Genetic analysis and functional characterization of the *Streptococcus pneumoniae* vic operon. *Infect Immun.* **2002**;70(11):6121–6128. doi: [10.1128/IAI.70.11.6121-6128.2002](https://doi.org/10.1128/IAI.70.11.6121-6128.2002)
- [41] Lei L, Zhang B, Mao M, et al. Carbohydrate metabolism regulated by antisense vicR RNA in cariogenicity. *J Dent Res.* **2020**;99(2):204–213. doi: [10.1177/0022034519890570](https://doi.org/10.1177/0022034519890570)
- [42] Deng DM, Liu MJ, ten Cate JM, et al. The VicRK system of *Streptococcus mutans* responds to oxidative stress. *J Dent Res.* **2007**;86(7):606–610. doi: [10.1177/154405910708600705](https://doi.org/10.1177/154405910708600705)
- [43] Abranches J, Chen Y-Y, Burne RA. Characterization of *Streptococcus mutans* strains deficient in EIIAB man of the sugar phosphotransferase system. *Appl Environ Microbiol.* **2003**;69(8):4760–4769. doi: [10.1128/AEM.69.8.4760-4769.2003](https://doi.org/10.1128/AEM.69.8.4760-4769.2003)
- [44] Fozo EM, Scott-Anne K, Koo H, et al. Role of unsaturated fatty acid biosynthesis in virulence of

- Streptococcus mutans*. *Infect Immun*. 2007;75(3):1537–1539. doi: 10.1128/IAI.01938-06
- [45] Ye XL, Xu L, Li XG, et al. Antibacterial mechanism of houttuynonate homologues against *Bacillus subtilis*. *Colloids Surfaces A-Physicochem Eng Aspects*. 2009;350(1–3):130–135. doi: 10.1016/j.colsurfa.2009.09.017
- [46] Wang T, Huang W, Duan Q, et al. Sodium houttuynonate in vitro inhibits biofilm dispersion and expression of *bdIA* in *Pseudomonas aeruginosa*. *Mol Biol Rep*. 2019;46(1):471–477. doi: 10.1007/s11033-018-4497-9
- [47] Wu D, Huang W, Duan Q, et al. Sodium houttuynonate affects production of N-acyl homoserine lactone and quorum sensing-regulated genes expression in *Pseudomonas aeruginosa*. *Front Microbiol*. 2014;5:635.
- [48] Do LG. Guidelines for use of fluorides in Australia: update 2019. *Aust Dent J*. 2020;65(1):30–38. doi: 10.1111/adj.12742
- [49] Zhang TT, Guo HJ, Liu XJ, et al. *Galla chinensis* compounds remineralize enamel caries lesions in a rat model. *Caries Res*. 2016;50(2):159–165. doi: 10.1159/000445036
- [50] Jiang W, Peng J, Jiang N, et al. Chitosan phytate nanoparticles: a synergistic strategy for effective dental caries prevention. *ACS Nano*. 2024;18(21):13528–13537. doi: 10.1021/acsnano.3c11806
- [51] Liao Y, Brandt BW, Li J, et al. Fluoride resistance in *Streptococcus mutans*: a mini review. *J Oral Microbiol*. 2017;9(1):1344509. doi: 10.1080/20002297.2017.1344509
- [52] Ullah R, Zafar MS, Shahani N. Potential fluoride toxicity from oral medicaments: a review. *Iran J Basic Med Sci*. 2017;20(8):841–848. doi: 10.22038/IJBMS.2017.9104
- [53] Rahim ZHA, Khan HBSG. Comparative studies on the effect of crude aqueous (CA) and solvent (CM) extracts of clove on the cariogenic properties of *Streptococcus mutans*. *J Oral Sci*. 2006;48(3):117–123. doi: 10.2334/josnurd.48.117
- [54] Chau NPT, Pandit S, Jung JE, et al. Evaluation of *Streptococcus mutans* adhesion to fluoride varnishes and subsequent change in biofilm accumulation and acidogenicity. *J Dent*. 2014;42(6):726–734. doi: 10.1016/j.jdent.2014.03.009
- [55] Zhi C, Chen X, Yu K, et al. A bifunctional nanocomplex with remineralizing and antibacterial activities to interrupt dental caries. *J Control Release*. 2024;376:717–731. doi: 10.1016/j.jconrel.2024.10.041
- [56] Wu S, Huang F, Zhang H, et al. *Staphylococcus aureus* biofilm organization modulated by YycFG two-component regulatory pathway. *J Orthop Surg Res*. 2019;14(1):10. doi: 10.1186/s13018-018-1055-z
- [57] Ng WL, Robertson GT, Kazmierczak KM, et al. Constitutive expression of PcsB suppresses the requirement for the essential VicR (YycF) response regulator in *Streptococcus pneumoniae* R6 Δ . *Mol Microbiol*. 2003;50(5):1647–1663. doi: 10.1046/j.1365-2958.2003.03806.x
- [58] Zhang Y, Xie X, Ma W, et al. Multi-targeted antisense oligonucleotide delivery by a framework nucleic acid for inhibiting biofilm formation and virulence. *Nano-Micro Lett*. 2020;12(1):74. doi: 10.1007/s40820-020-0409-3
- [59] Liu C, Zhang H, Peng X, et al. Small molecule attenuates bacterial virulence by targeting conserved response regulator. *MBio*. 2023;14(3):e0013723. doi: 10.1128/mbio.00137-23